Chemical Physics Letters 762 (2021) 138106

Contents lists available at ScienceDirect

Chemical Physics Letters

journal homepage: www.elsevier.com/locate/cplett

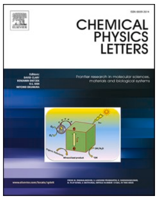

Research paper

Unraveling a trifecta of weak non-covalent interactions: The dissociation energy of the anisole-ammonia 1:1 complex

John L. Loman, James T. Makuvaza, Damian L. Kokkin, Scott A. Reid *

Department of Chemistry, Marquette University, Milwaukee, WI 53233, United States

A B S T R A C T

The anisole-ammonia 1:1 complex is a challenge for both experiment and theory. Early studies supported a non-planar structure, involving a trifecta of weak non-covalent interactions: N-H/O, N-H/π, and C-H/N. The calculated structure and binding energy of the complex proved remarkably sensitive to the level of theory employed. Here, we report the first experimental measurement of the ground state dissociation energy of the complex, and derive an excited (S_1) state dissociation energy that is in excellent agreement with the cutoff observed in the experimental excitation spectrum. Results are compared with previous predictions and new calculations based on benchmarked Density Functional Theory methods.

1. Introduction

Complexes of aromatic chromophores with various solvents have long been used as model systems to probe weak non-covalent interactions [1–3], as these interactions emulate a plethora of real-world occurrences, e.g., in supramolecular chemistry [4,5], molecular recognition and sensing [6], and catalysis [7]. Experimental study of the structure and dissociation energies of such complexes provides valuable benchmark data for theoretical approaches [8–10], and provides insight into competitive or cooperative non-covalent binding interactions [11,12]. A complex of particular interest that has provided a challenge for theory is the anisole–NH_3 1:1 complex.

In 2007, Piani *et al.* examined this complex using resonant two-photon ionization (R2PI) spectroscopy [13]. The origin transition was red-shifted from the bare anisole origin by ~200 cm^{-1}, a feature often characteristic of π-type non-covalent interactions with an aromatic system [14]. This stands in contrast to the structure of the related phenol-ammonia 1:1 complex, which shows a planar hydrogen–bonded complex [15]. Based upon the observed low resolution rotational contour of the origin band, the observed complex was indeed assigned to a π-type complex, exhibiting a trifecta of N-H/π, N-H/O, and C-H/N interactions with the aromatic ring and methoxy group. Foreshadowing the difficulties in theoretical treatment of this system, calculations at the B3LYP/6-311++G** level revealed three minima on the Potential Energy Surface (PES), with the in-plane H-bonded structure predicted to have the largest stabilization energy.

Shortly thereafter, the same group reported high resolution Laser Induced Fluorescence (LIF) spectra of the complex and with the Barone group carried out extensive theoretical calculations [16]. The rotationally resolved spectrum confirmed the previous assignment, and new theoretical calculations using MP2 and dispersion-corrected DFT methods showed that the non-planar complex was indeed the global minimum energy structure. However, these methods gave disparate values for the complex binding energy. In 2008, Barone and co-workers reported more extensive theoretical studies of the binding energy in the S_0 and S_1 states [17], showing that the structure of the complex was very sensitive to the level of theoretical treatment, with DFT and MP2 optimized structures displaying significant differences. As a result, the calculated S_0 binding energies using these methods varied over a wide range, from ~4 to ~13 kJ/mol. For the S_1 state, the results were even more dramatic, as TD-DFT methods gave binding energies as high as 22 kJ/mol, while EOM-CCSD predictions were much smaller, of order 4–7 kJ/mol. In 2009, Giuliano *et al.* performed a study of the complex using microwave spectroscopy [18]. The experimental rotational constants were well reproduced from a structure optimized at the MP2/6-311++G** level, from which a ground state binding energy of 9.0 kJ/mol (corrected for ZPE and BSSE using the counterpoise method) was predicted.

To data, there has not been an experimental measurement of the dissociation energy of the complex in the S_0 or S_1 states. Given the sensitivity of the calculated binding energy to level of theory, basis set, and dispersion correction, such a measurement is highly desirable. In this letter, we report experimental determination of the S_0 binding energy for the anisole-(NH_3) 1:1 complex using 2-color appearance potential (2CAP) spectroscopy. The derived value is in good agreement with benchmarked theoretical methods, and the S_1 state binding energy

---

* Corresponding author.
E-mail address: scott.reid@marquette.edu (S.A. Reid).

https://doi.org/10.1016/j.cplett.2020.138106
Received 25 August 2020; Received in revised form 29 September 2020; Accepted 19 October 2020

derived from this measurement is in accord with the cutoff observed in the experimental R2PI spectrum. While not emphasized here, our calculations predict a large increase in binding energy in the D_0 state, consistent with partial formation of a C-N bond in a pre-reactive complex as has been observed in the related halobenzene-ammonia complexes [19–21].

2. Experimental and computational details

All experimental work was performed using a time-of-flight mass spectrometer described in detail elsewhere [11,20–23]. To generate the anisole-(NH_3) 1:1 complex, a premix of ~1% ammonia in argon was passed over a bubbler of liquid anisole held in a −5 °C bath. The gaseous mixture was expanded into the source chamber of the mass spectrometer through a 0.8 mm opening of a pulsed valve nozzle (General Valve series 9) and then skimmed by a 1.5 mm skimmer (Beam Dynamics) prior to entering the ionization region. Excitation of the complex was achieved by the frequency-doubled output of a Lambda Physik Scanmate dye laser, pumped by the third harmonic of a Quantel QSmart–850 Nd:YAG laser. After excitation, ionization of the complex was achieved by the output of a Sirah Cobra Stretch dye laser pumped by a Continuum Indi Nd:YAG laser. This ionization laser was aligned counterpropagating to the excitation laser and temporally overlapped, with the pulse delays controlled using an eight-channel delay generator (Berkeley Nucleonics 565).

Excitation spectra for the anisole monomer and 1:1 anisole–NH_3 complex were determined by setting the ionization laser (λ_2) above the ionization threshold, and scanning the frequency of the excitation laser (λ_1) while monitoring the onset of monomer or complex ion signal in the mass spectrum. To determine the S_0 state dissociation energy, 2CAP measurements were performed, where the pump laser was set on resonance (λ_1) of the 1:1 complex and the second (ionizing) laser (λ_2) scanned above the dissociation threshold while monitoring the mass channel of the anisole monomer cation [11].

Calculations were performed using the Gaussian 16 [24] suite of packages on the XSEDE *Comet* super-computing cluster [25]. Single-hybrid methods of B3LYP [26–29], CAM-B3LYP [30,31], PBE0 [32,33], PW6B95 [34], and M06-2X [35] were used in this work, combined with the def2-QZVPPD basis set [36,37] and Grimme's D3 dispersion term [38,39]. All structures were optimized with tight convergence criteria, and frequency calculations performed to identify minima on the potential energy surface. Calculated binding energies were corrected for zero-point energy (ZPE). With the basis set employed here, the overstabilization from BSSE was negligible (<0.2 kJ/mol).

3. Results and discussion

Fig. 1 shows the 2CR2PI excitation spectrum of the 1:1 anisole-NH_3 complex, with the energy axis defined with respect to the origin transition of anisole. The spectrum shows an origin band which is red–shifted from the anisole origin transition by 193 cm^{-1}, in agreement with prior studies [13]. In the overview spectrum (upper panel), a clear cutoff in sharp vibronic structure is evidenced roughly 1000 cm^{-1} above the origin band. The region near the origin band (lower panel) shown extensive vibronic activity which can largely be assigned to fundamentals, overtones, and combination bands involving two intermolecular vibrations with harmonic frequencies of 34 and 39 cm^{-1}, respectively (Table S1).

Subsequently, we carried out two-color appearance potential (2CAP) measurements [9]. Here the appearance energy of the anisole cation radical fragment is approximated as the sum of the ground state dissociation energy of the anisole–NH_3 1:1 complex and the ionization potential of anisole. The 2CAP spectrum, with the anisole ionization potential subtracted so that the x-axis is a direct readout of the ground (S_0) state dissociation energy, is shown in Fig. 2. This spectrum displays two onsets, with the second onset lying approximately 11.4 kJ/mol (or 950 cm^{-1}) higher in energy than the first. As this difference corresponds closely to the vibrational frequency of the wagging mode in ammonia, we assign the first onset to the formation of vibrationally cold ammonia fragments, and the second to the appearance of vibrationally excited fragments. The initial onset corresponds to an upper limit of the ground (S_0) state dissociation energy of 10.2(7) kJ/mol.

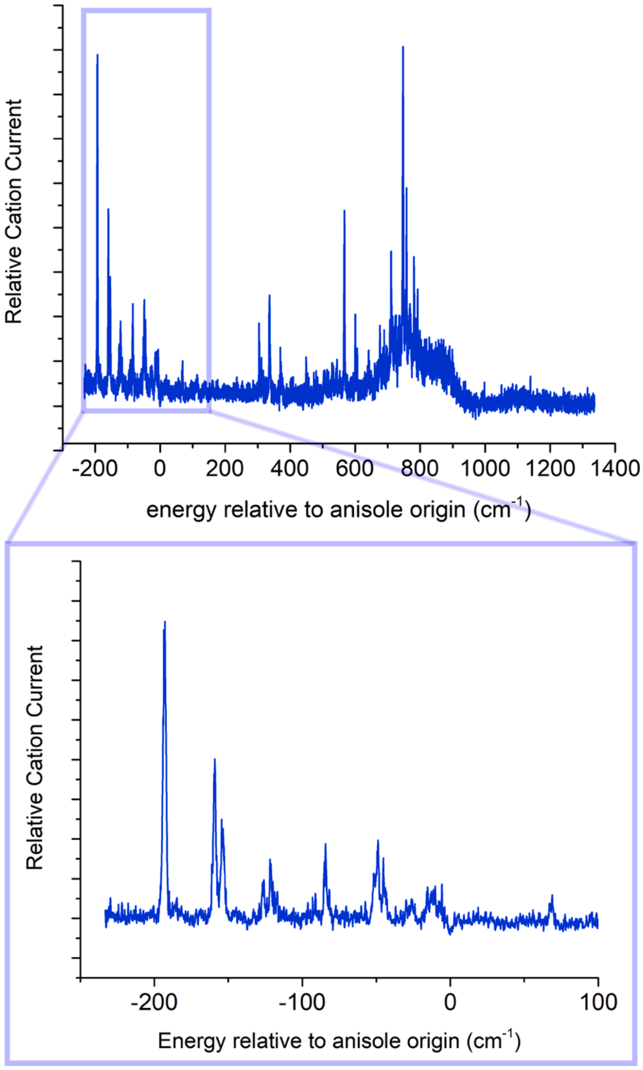

Fig. 1. The R2PI spectrum of the anisole-(NH_3) 1:1 complex obtained by scanning the excitation laser with fixed wavelength ionization laser while monitoring the complex mass channel. The energy scale is given relative to the origin of the anisole S_0-S_1 spectrum. The inset shows an expanded view of the region near the origin.

As a check on the 2CAP derived value, we combined this value with the observed spectral red-shift for the complex (Fig. 1) to derive a dissociation energy in the S_1 state. This calculation returned an S_1 state dissociation energy of 12.6(7) kJ/mol. In Fig. 3, this predicted value is compared with the S_0-S_1 excitation spectrum in the region where the breakoff in sharp structure is observed. Here we have re-referenced the x-axis to reflect energy relative to the origin band of the complex. It is clear from this figure that the derived binding energy, represented as an X with associated error bar on the energy axis, is consistent with the observed spectral cutoff, which presumably represents the onset of rapid dissociation in the S_1 state.

With experimental dissociation energies derived for the S_0 [10.2(7) kJ/mol] and S_1 [12.6(7) kJ/mol] states, we return to the detailed calculations reported by Barone and co-workers [17]. Our S_0 value is closest to the predicted value (11.3 kJ/mol) at the M05-2X/6-311+G(d,

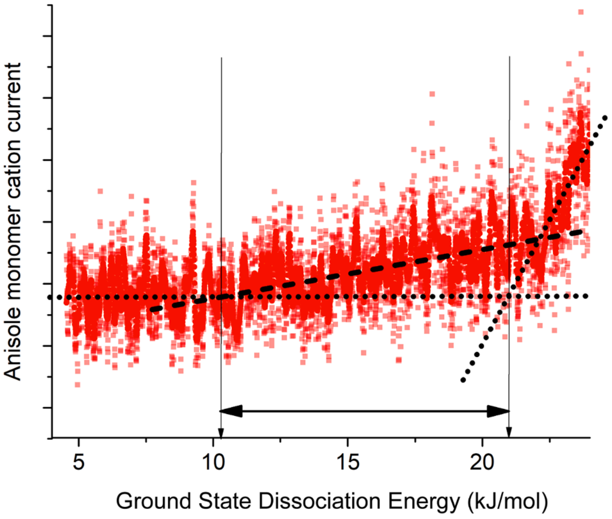

Fig. 2. The 2CAP spectrum for the 1:1 anisole–NH_3 complex with energy axis referenced to give directly the ground (S_0) state dissociation energy. The second onset is assigned to the formation of vibrationally excited NH_3 fragments. The darker line in this figure represents a 10-point smoothing of the raw data (dots).

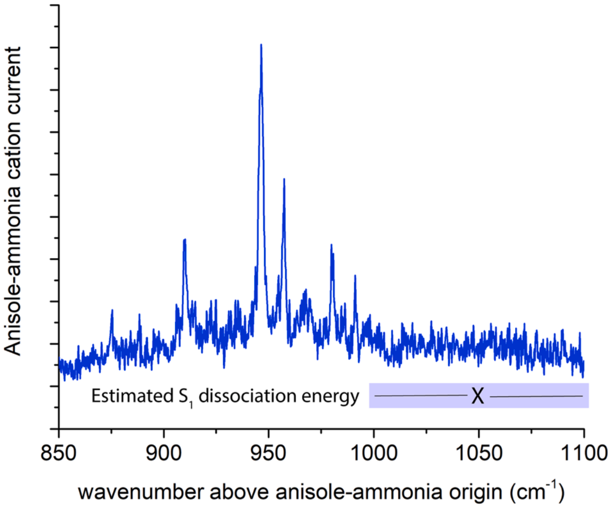

Fig. 3. Expanded view of the 2CR2PI spectrum in the region of the cutoff in sharp vibronic structure. As indicated, this cutoff is consistent with the S_1 dissociation energy estimated from the 2CAP measurement and the observed spectral red-shift in the S_0-S_1 spectrum of the complex.

p) level, while our derived S_1 value is close to predicted values at the TD-B3LYP-DM/6-311+G(d,p) (13.8 kJ/mol) and TD-LC-ωPBE/6-311+G(d,p) (11.6 kJ/mol) levels. To further understand the intriguing trifecta of non-covalent interactions in this system, we carried out calculations as described above. Our calculated structures were consistent with prior studies in revealing three modes of non-covalent interactions: N-H···π, N-H···O, and C-H···N, as illustrated in Figure S1, which displays the optimized structures at five different levels of theory. Table 1 indicates the ground state (S_0) dissociation energy estimated from the dispersion corrected DFT methods used in this work. All gave values in reasonable agreement with experiment.

Finally, while not the focus of this work, it is interesting to note that the binding energy in the D_0 state as predicted by theory is significantly increased in comparison with S_0 and S_1. For example, calculations at the UPBEO-D3/aug-cc-pVTZ level predict a binding energy of roughly 40 kJ/mol, and a structure where the ammonia has moved over the α-carbon, forming an incipient bond. This is reminiscent of related complexes of halobenzenes with ammonia, where upon ionization the ammonia attacks the electrophilic α-carbon, leading to the formation of Wheland intermediates which react via halogen atom or hydrogen halide loss [19,21].

Table 1
Experimental dissociation energy compared with calculated binding energies of the ground state of the 1:1 anisole ammonia complex.

Anisole-(NH_3) S_0 dissociation energy calculations	
Method	Energy (kJ/mol)
Experimental dissociation energy	10.2(7)
PW6B95-D3/def2-QZVPPD	9.9
B3LYP-D3/def2-QZVPPD	11.6
CAM-B3LYP-D3/def2-QZVPPD	11.8
PBE0-D3/def2-QZVPPD	12.1
M06-2X-D3/def2-QZVPPD	12.3

4. Conclusions

The anisole–NH_3 1:1 complex has proven a challenging system for theory, with predictions of the ground state binding energy varying over a wide range. Here, we have determined experimentally an upper limit to the dissociation energy for the anisole–NH_3 1:1 complex in the ground state, 10.2(7) kJ/mol. From this value, the inferred S_1 state binding energy is in excellent agreement with the observed cutoff in the excitation spectrum. The calculated minimum energy structure shows a complicated interplay of three types of non-covalent interactions; N-H···O, N-H···π, and C-H···N interactions. Our experimentally measured value is in reasonable agreement with benchmarked and dispersion-corrected DFT methods. Overall, this system is an excellent one for exploring cooperativity and competition amongst weak non-covalent interactions.

CRediT authorship contribution statement

John L. Loman: Investigation, Formal analysis, Writing - original draft. **James T. Makuvaza:** Writing - review & editing, Formal analysis. **Damian L. Kokkin:** Writing - review & editing, Supervision. **Scott A. Reid:** Writing - review & editing, Supervision, Project administration, Funding acquisition.

Declaration of Competing Interest

The authors declare that they have no known competing financial interests or personal relationships that could have appeared to influence the work reported in this paper.

Acknowledgements

This work used the Extreme Science and Engineering Discovery Environment (XSEDE) *Comet* super-computing cluster, which is supported by National Science Foundation grant number ACI-1548562. The authors thank Dr. Qadir Timerghazin for helpful advice.

Appendix A. Supplementary data

Supplementary data to this article can be found online at https://doi.org/10.1016/j.cplett.2020.138106.

References

[1] T. Ebata, A. Fujii, N. Mikami, Vibrational spectroscopy of small-sized hydrogen-bonded clusters and their ions, Int. Rev. Phys. Chem. 17 (3) (1998) 331–361.

[2] L.L. Connell, S.M. Ohline, P.W. Joireman, T.C. Corcoran, P.M. Felker, Rotational coherence spectroscopy and structure of phenol dimer, J. Chem. Phys. 96 (4) (1992) 2585–2593.

[3] E.J. Bieske, M.W. Rainbird, A.E.W. Knight, The Vanderwaals vibrations of aniline (Argon)2 in the S1 electronic state, J. Chem. Phys. 94 (11) (1991) 7019–7028.

[4] H.W. Roesky, M. Andruh, The interplay of coordinative, hydrogen bonding and pi-pi stacking interactions in sustaining supramolecular solid-state architectures. A study case of bis(4-pyridyl)- and bis(4-pyridyl-N-oxide) tectons, Coordin. Chem. Rev. 236 (1–2) (2003) 91–119.

[5] P. Metrangolo, F. Meyer, T. Pilati, G. Resnati, G. Terraneo, Halogen bonding in supramolecular chemistry, Angew. Chem. Int. Ed. 47 (33) (2008) 6114–6127.

[6] H.-Q. Wei, W.-J. Jin, Applications of halogen bonding in chemical sensing and molecular recognition, Fenxi Huaxue 35 (11) (2007) 1381–1386.

[7] K.T. Mahmudov, A.V. Gurbanov, F.I. Guseinov, M.F.C.G. da Silva, Noncovalent interactions in metal complex catalysis, Coordin. Chem. Rev. 387 (2019) 32–46.

[8] K.S. Kim, P. Tarakeshwar, J.Y. Lee, Molecular clusters of pi-systems: theoretical studies of structures, spectra, and origin of interaction energies, Chem. Rev. 100 (11) (2000) 4145–4185.

[9] J.A. Frey, C. Holzer, W. Klopper, S. Leutwyler, Experimental and theoretical determination of dissociation energies of dispersion-dominated aromatic molecular complexes, Chem. Rev. 116 (9) (2016) 5614–5641.

[10] S.R. Gadre, S.D. Yeole, N. Sahu, Quantum chemical investigations on molecular clusters, Chem. Rev. 114 (24) (2014) 12132–12173.

[11] J.T. Makuvaza, D.L. Kokkin, J.L. Loman, S.A. Reid, C-H/pi and C-H-O interactions in concert: a study of the anisole-methane complex using resonant ionization and velocity mapped ion imaging, J. Phys. Chem. A 123 (13) (2019) 2874–2880.

[12] J.T. Makuvaza, J.L. Loman, D.L. Kokkin, S.A. Reid, Probing cooperativity in C-HN and C-H pi interactions: dissociation energies of aniline(CH4)(n) (n=1, 2) van der Waals complexes from resonant ionization and velocity mapped ion imaging measurements, J. Chem. Phys. 153 (4) (2020).

[13] G. Piani, M. Pasquini, G. Pietraperzia, M. Becucci, A. Armentano, E. Castellucci, The anisole-ammonia complex: marks of the intermolecular interactions, Chem. Phys. Lett. 434 (1–3) (2007) 25–30.

[14] N.M. Tonge, E.C. MacMahon, I. Pugliesi, M.C.R. Cockett, The weak hydrogen bond in the fluorobenzene-ammonia van der Waals complex: Insights into the effects of electron withdrawing substituents on pi versus in-plane bonding, J. Chem. Phys. 126 (15) (2007).

[15] C. Crepin, A. Tramer, Electronic-spectra and proton-transfer in the phenol (Nh3)N clusters in argon matrices, Chem. Phys. 156 (2) (1991) 281–291.

[16] M. Biczysko, G. Piani, M. Pasquini, N. Schiccheri, G. Pietraperzia, M. Becucci, M. Pavone, V. Barone, On the properties of microsolvated molecules in the ground (S-0) and excited (S-1) states: the anisole-ammonia 1: 1 complex, J. Chem. Phys. 127 (14) (2007).

[17] V. Barone, M. Biczysko, M. Pavone, The role of dispersion correction to DFT for modelling weakly bound molecular complexes in the ground and excited electronic states, Chem. Phys. 346 (1–3) (2008) 247–256.

[18] B.M. Giuliano, A. Maris, S. Melandri, W. Caminati, Pure rotational spectrum and model calculations of anisole-ammonia, J. Phys. Chem. A 113 (52) (2009) 14277–14280.

[19] S. Nyambo, B. Uhler, L. Muzangwa, M. Ivanov, B.K. Welch, R. Dawes, S.A. Reid, Reactive pathways in the bromobenzene-ammonia dimer cation radical: evidence for a roaming halogen radical, J. Mol. Struct. 1172 (2018) 113–118.

[20] L. Muzangwa, S. Nyambo, B. Uhler, S.A. Reid, On pi-stacking, C-H/pi, and halogen bonding interactions in halobenzene clusters: resonant two-photon ionization studies of chlorobenzene, J. Chem. Phys. 137 (18) (2012) 184307.

[21] S.A. Reid, S. Nyambo, A. Kalume, B. Uhler, C. Karshenas, L. Muzangwa, Reactive pathways in the chlorobenzene-ammonia dimer cation radical: new insights from experiment and theory, J. Phys. Chem. A 117 (47) (2013) 12429–12437.

[22] S.A. Reid, S. Nyambo, L. Muzangwa, B. Uhler, pi-Stacking, C-H/pi, and halogen bonding interactions in bromobenzene and mixed bromobenzene-benzene clusters, J. Phys. Chem. A 117 (50) (2013) 13556–13563.

[23] S.A. Reid, S. Nyambo, L. Muzangwa, B. Uhler, π-stacking, C-H/π, and halogen bonding interactions in bromobenzene and mixed bromobenzene-benzene clusters, J. Phys. Chem. A (2013) (in press).

[24] M.J. Frisch, et al., Gaussian 16, Revision B.01, Gaussian: Wallingford CT, 2016.

[25] J. Towns, T. Cockerill, M. Dahan, I. Foster, K. Gaither, A. Grimshaw, V. Hazlewood, S. Lathrop, D. Lifka, G.D. Peterson, R. Roskies, J.R. Scott, N. Wilkins-Diehr, XSEDE: accelerating scientific discovery, Comput. Sci. Eng. 16 (5) (2014) 62–74.

[26] S.H. Vosko, L. Wilk, M. Nusair, Accurate spin-dependent electron liquid correlation energies for local spin-density calculations - a critical analysis, Can. J. Phys. 58 (8) (1980) 1200–1211.

[27] C.T. Lee, W.T. Yang, R.G. Parr, Development of the Colle-Salvetti correlation-energy formula into a functional of the electron-density, Phys. Rev. B 37 (2) (1988) 785–789.

[28] A.D. Becke, Density-functional thermochemistry.3. The role of exact exchange, J. Chem. Phys. 98 (7) (1993) 5648–5652.

[29] P.J. Stephens, F.J. Devlin, C.F. Chabalowski, M.J. Frisch, Ab-initio calculation of vibrational absorption and circular-dichroism spectra using density-functional force-fields, J. Phys. Chem. 98 (45) (1994) 11623–11627.

[30] M.J.G. Peach, T. Helgaker, P. Salek, T.W. Keal, O.B. Lutnaes, D.J. Tozer, N. C. Handy, Assessment of a Coulomb-attenuated exchange-correlation energy functional, Phys. Chem. Chem. Phys. 8 (5) (2006) 558–562.

[31] T. Yanai, D.P. Tew, N.C. Handy, A new hybrid exchange-correlation functional using the Coulomb-attenuating method (CAM-B3LYP), Chem. Phys. Lett. 393 (1–3) (2004) 51–57.

[32] J.P. Perdew, K. Burke, M. Ernzerhof, Generalized gradient approximation made simple, Phys. Rev. Lett. 77 (18) (1996) 3865–3868.

[33] J.P. Perdew, K. Burke, M. Ernzerhof, Generalized gradient approximation made simple (vol 77, pg 3865, 1996), Phys. Rev. Lett. 78 (7) (1997) 1396.

[34] Y. Zhao, D.G. Truhlar, Design of density functionals that are broadly accurate for thermochemistry, thermochemical kinetics, and nonbonded interactions, J. Phys. Chem. A 109 (25) (2005) 5656–5667.

[35] Y. Zhao, D.G. Truhlar, The M06 suite of density functionals for main group thermochemistry, thermochemical kinetics, noncovalent interactions, excited states, and transition elements: two new functionals and systematic testing of four M06-class functionals and 12 other functionals, Theor. Chem. Acc. 120 (1–3) (2008) 215–241.

[36] F. Weigend, F. Furche, R. Ahlrichs, Gaussian basis sets of quadruple zeta valence quality for atoms H-Kr, J. Chem. Phys. 119 (24) (2003) 12753–12762.

[37] D. Rappoport, F. Furche, Property-optimized Gaussian basis sets for molecular response calculations, J. Chem. Phys. 133 (13) (2010).

[38] S. Grimme, S. Ehrlich, L. Goerigk, Effect of the damping function in dispersion corrected density functional theory, J. Comput. Chem. 32 (7) (2011) 1456–1465.

[39] S. Grimme, J. Antony, S. Ehrlich, H. Krieg, A consistent and accurate ab initio parametrization of density functional dispersion correction (DFT-D) for the 94 elements H-Pu, J. Chem. Phys. 132 (15) (2010).